Use of Electrochemical Techniques to Evaluate the Effect of Red Mud Addition on the Corrosion of Reinforced Concrete

Daniel.V. Ribeiro[a]; Carlos A.D. Rovere[b]; Sebastião E. Kuri[c]; João A. Labrincha[d]; João C.C. Abrantes[e]; Márcio R. Morelli[f]

Abstract

The corrosion of concrete reinforcement is a worldwide problem with serious consequences to humans, including accidental deaths that may occur due to the degradation of this material. Thus, techniques that can measure concrete reinforcement corrosion and provide a reliable prediction of this phenomenon are fundamental for the technological development of these materials. The corrosion of steel bars embedded in concrete containing varying amounts of red mud (up to 30% of the total binder) was tested by EIS and electrical resistivity, under partial immersion in a sodium chloride solution. The high pH also provides greater protection of rebars, which is reflected in the high electrical resistivity (filler effect) of concrete and the addition of red mud delayed the onset of corrosion and possibly also reduced the corrosion rate.

Keywords: corrosion, reinforcement, red mud, electrochemical impedance spectroscopy, electrochemical property.

Introduction

The global production of bauxite in 2009 was 205 million tons, and the main producing countries were Australia, China, Brazil, Guinea, India and Jamaica. Occupying the third position in the world ranking in 2009, Brazil produced 26.6 million tons of bauxite. It also has the world's third largest bauxite ore reserves (around 3.5 billion tons), concentrated mainly in the north of the country (state of Pará) (1). Roughly (0.3 – 1.0) tons of red mud are generated for each ton of aluminum produced. About 10.6 million tons of caustic red mud have been discarded annually during recent years in Brazil and the global generation of red mud exceeds 117 million tons/year (2).

Alkaline matrices such as that ensured by Portland cement in mortars and concrete are commonly used in waste conditioning. They are inexpensive, show an extensively documented history of safe use, and are a readily accessible technology. Alkalinity greatly reduces the solubility of many hazardous inorganic species and inhibits microbiological

[a] PhD, Civil and Materials Engineer / Federal University of Bahia – UFBA, Brazil
[b] PhD, Materials Engineer / Federal University of São Carlos – UFSCar, Brazil
[c] PhD, Materials Engineer / Federal University of São Carlos – UFSCar, Brazil
[d] PhD, Materials Engineer / University of Aveiro, Portugal
[e] PhD, Materials Engineer / Polytechnic Institute of Viana do Castelo, Portugal
[f] PhD, Materials Engineer / Federal University of São Carlos – UFSCar, Brazil

processes. Moreover, since these matrices require water for hydration, they may readily incorporate wet wastes (1) such as red mud.

The search for an economically and environmentally viable alternative has led to the study of red mud in various applications, e.g., as an adsorbent for removing heavy metals from aqueous solutions (3), as a stabilizing material for clay liners (4), red mud–polymer composites panels as a substitute for wood (5), building materials, i.e., bricks (6), ceramics and tiles (7), ceramic glazes (8), and iron-rich cement (9, 10).

The high alkalinity of red mud, which was initially a factor of environmental concern, now emerges as a major asset in the attempt to use red mud as an inhibitor of reinforced concrete rebar corrosion by retaining its passivity. To evaluate this possibility, rebar corrodibility was examined by the electrochemical impedance spectroscopy (EIS) and electrical resistivity techniques.

Methods

Characterization of Materials and Preparation of Concrete Samples

The materials were characterized by X-ray diffraction (Rigaku Geigerflex ME 210GF2 diffractometer) and X-ray fluorescence spectroscopy (Philips PW 1480 XRF spectrometer), while physical parameters such as specific surface area (estimated by BET, using a Micrometrics Gemini 2370 V1.02 analyzer) and specific gravity (Micrometrics Helium Pycnometer Accupyc 1330 V2.01) were also determined.

Concrete was prepared with ordinary Portland cement and red mud mixed in the following proportions: 1.0 (Portland cement): 1.5 (fine aggregate): 1.3 (coarse aggregate) and a water/cement ratio of 0.5. Red mud was added in partial substitution of Portland cement in the proportions of: 10 %, 20 % and 30 % (weight). The mortar content was 75 % and the cement consumption was 526 kg/m^3. Samples without red mud (reference) were also prepared.

Two commercial steel rebars (Gerdau, type CA-50) with a diameter of 6.3 mm were embedded in each prismatic concrete block (50 mm x 70 mm x 90 mm) with a concrete topping of 2.25 cm (Figure 1). With this geometry, the distance between the inner surfaces of the steel rebars was 2.5 cm and the exposed embedded area of each electrode was 15.83 cm^2. The electrical resistivity of the concrete was tested using molded concrete blocks (200 mm x 200 mm x 100 mm) with sensors embedded in them.

Concrete blocks were demolded 24 h after being cast and were cured for 4 weeks in a saturated humidity chamber before immersion in the aggressive solutions.

Electrochemical Impedance Spectroscopy (EIS)

The prismatic concrete specimens were subjected to monthly cycles of oven drying (one week) and partial immersion in a 3 % sodium chloride (NaCl) solution (three weeks). Three specimens of each composition were tested and an average of six results (two rebars per sample) is presented.

Before starting each measurement, the cell was assembled using the saturated calomel electrode (SCE, Hg/Hg_2SO_4 sat K_2SO_4) as reference and the counter electrode (carbon) was placed on the concrete surface, providing a wet sponge to assure a good electrolytic contact, with the rebars serving as the working electrodes.

The EIS measurements were taken with a Solartron 1287A potentiostat/galvanostat and a Solartron 1260 impedance analyzer, both monitored by computer with ZPlot/CorrWare V. 2.3 software. The parameters used in this impedance scan were:

- Initial frequency: 50 kHz,
- Final frequency: 10 mHz,
- Amplitude (rms): 5 mV,
- Ambient temperature: (23 ± 2) ºC,
- Current range: 1 A a 100 nA,
- Electrochemical potential: Ecorr,
- Total time for each test: 30 min.

The results were analyzed using ZView 2 software. Measurements were taken at 30-day intervals for the first three months and at 60-day intervals thereafter. Thus, measurements were taken at 1, 2, 3, 5, 7, 9, 11 and 13 months of age. A minimum of three samples (6 electrodes) were tested in all determinations. Figure 2 illustrates the setup of the test apparatus to measure the corrosion process by EIS.

Electrical Resistivity

The electrical resistivity of concrete was calculated from the electrical current (I) passing through the specimens. The system, which is shown schematically in Figure 3, consists of two cylindrical probes, each with two electrodes (different measurement levels) made of stainless steel (rings/washers) and spaced at different layer depths. The probes used in this study were supplied by the Institute of Corrosion (ICorr), which is specialized in corrosion studies. The two probes of the system should be placed 10 cm apart.

Through this monitoring system, the ionic resistivity of concrete at each depth can be determined by the paired-electrode technique. An alternating current is applied between the electrodes and the resistivity is determined by measuring the resistance (ΔE/ΔI, Ohm's law) and by a parameter that depends on the geometry of the electrodes and on the distance between them (A/L). Thus, the resistivity (ρ) is calculated according to equation (A):

$$\rho = \frac{V \cdot A}{I \cdot L} \qquad \text{(A)}$$

For circular electrodes, equation (A) is equivalent to:

$$\rho = \frac{2\pi \cdot V \cdot L}{I} \qquad \text{(B)}$$

where ρ is the electrical resistivity of concrete (Ω.cm); V is the applied voltage; I is the current intensity; A is the area of the side of the specimen in contact with the electrode (cm^2); and L is the distance between the electrodes (cm). The European CE Bulletin – COST 509 (Corrosion and Protection of Metals in Contact with Concrete) was used as the evaluation parameter since it is more stringent in relation to values than those suggested by the CEB-192 standard.

Results and discussion

Materials Characterization

The Portland cement used here had a specific surface area of 0.93 m^2/g and a specific gravity of 3.11 kg/dm^3. The sand had a specific surface area of 0.68 m^2/g and a specific gravity of 2.70 kg/dm^3, classified by the Brazilian NBR 7211 standard as fine sand. The gravel had a specific gravity of 2.74 kg/dm^3 and a maximum dimension of 19 mm.

The red mud was received in the form of paste containing about 40 % of free water. In the present study, the material was dried and crushed, and then used as a powdered additive. Ideally, to demonstrate its potential as a concrete constituent, red mud should be tested in the as-received condition; hence, the free water present in the mud should be considered a mortar mix component.

The red mud had a specific surface area of 20.27 m^2/g, as indicated by the particle fineness shown in Figure 4. Maximum particle size was under 40 µm and the mean value was only about 8 µm. Its specific gravity was 2.90 kg/dm^3 and its pH was very high (12.95), exceeding the limit (12.5) established by the Brazilian NBR 10004 standard for non-hazardous wastes.

Table 1 presents the chemical composition of the waste, while Figure 5 shows the corresponding XRD pattern. As expected, the predominant crystalline components were aluminium hydroxide ($Al(OH)_3$), calcium carbonate ($CaCO_3$), and iron oxide (Fe_2O_3), but relative amounts of SiO_2, muscovite and FeO(OH) were also relevant. Some of those oxides were also detected by XRD, in addition to aluminium hydroxide and a complex $Na_5Al_3CSi_3O_{15}$ phase.

Electrochemical Impedance Spectroscopy (EIS).

Initially, EIS measurements were taken every 30 days. However, after the first three months of analysis, this interval was increased to two months. Thus, measurements were taken at 1, 2, 3, 5, 7, 9, 11 and 13 months of age. A minimum of 3 samples (6 electrodes) were tested in all determinations. For purposes of clarity, the graphs of only one of these measurements for each red mud content and at each age are presented (the results closest to the average and hence the most representative ones were chosen). The results are shown in Figure 6.

In the Nyquist diagrams obtained, it is note that most of the spectra show similar characteristics: two incomplete arcs in different frequency regions. A time constant RC related to these arcs is represented by elements of an electrical circuit (resistor in parallel with a capacitor). In some cases the formation of a third arc was observed, making the interpretation of the results more complex and raising doubts about the associated phenomena.

To obtain information from EIS measurements requires a physical model of the system that allows the equivalent circuit elements to be correlated with their properties and with the description of the phenomena. Based on the characteristics of the material (concrete) and the possibilities suggested in the literature, the equivalent circuit that best fits the results is proposed in Figure 7a, where R_0, R_2 and R_e represent, respectively, the "offset resistance" (high frequencies), the concrete bulk resistance (medium frequencies) and the electrode resistance (low frequency). Thus, R_e represents the corrosion phenomenon in steel rebars. Note that the R_0 value is usually neglected and R_b ($R_b = R_0 + R_2$) is considered the typical concrete bulk corrosion resistance.

The analysis of the data became increasingly complex starting from the measurements in the seventh month, when the degree of corrosion was already considerable, due to overlapping phenomena and to noise in the measurement resulting from the heterogeneity of the samples.

In view of these difficulties, we decided to change the way in which the analysis was performed. The basic theory states that these processes have a characteristic angular relaxation frequency, w (starting from which they no longer respond), which is given by w = 1/RC and which can also be read graphically at the top of the arc of the impedance spectrum (17, 18). Thus, we sought to associate the analyzable arcs with the typical capacitances and frequencies of each phenomenon.

The identified arcs were therefore isolated and related to each of the phenomena and a local analysis was performed, which improved the accuracy. A similar strategy was adopted by Vermoyal *et al.* (17) in their studies. To this end, we used the simplified circuit shown in Figure 7b.

When arcs are analyzed separately and fitted according to the simplified electrical circuit (Figure 7b), one obtains the following results: the arc resistance (R''), the values of the constant phase element (CPE), Q, and the "n" index. This index measures the perfection of this element, varying between 0 and 1, and comes closer to the unit value as the CPE approaches a perfect capacitor, C (12-14). Thus, the characteristic capacitance, C, can be calculated according to equation (C).

$$C = Q^{\frac{1}{n}}.R^{\frac{1-n}{n}} \qquad \text{(C)}$$

The characteristic frequency (f) associated with this characteristic capacitance is calculated in Hertz, according to equations (D) and (E), where w = 1/RC (12, 15).

$$f(Hz) = \frac{w}{2\pi} \qquad \text{(D)}$$

$$f(Hz) = \frac{1}{2\pi.R.C} \qquad \text{(E)}$$

This correlation between the characteristic capacitances and characteristic frequencies calculated for each phenomenon is shown in Figure 8. The typical frequencies found for the specimens used in this study can be grouped as follows:

- Low frequencies in the range of 1 mHz to 10 Hz (10^{-3} Hz to 10 Hz) correspond to the electrode resistance (R_e) and are thus related to the corrosion phenomenon. The characteristic capacitance of this frequency band ranges from 10^{-6} F/cm^2 to 10^{-3} F/cm^2.

- Medium frequencies in the range of 100 Hz to MHz (10^2 Hz to 10^6 Hz) correspond to the concrete resistance (R_2) and are related to the characteristics of the concrete surrounding and protecting the rebar. The characteristic capacitance of this frequency band lies between 10^{-9} F/cm^2 and 10^{-6} F/cm^2.

- High frequencies above the MHz range (> 10^6 Hz) are associated with the "offset resistance" (R_0), whose relevance is minor and whose values were neglected in this study.

Values similar to those shown in Figure 8 have been reported by other authors (12). The results obtained for concrete corrosion resistance, R_b (Ω), for different red mud contents are given in Table 2.

As can be seen in Table 2, the concrete corrosion resistance, R_b, increased over time. A similar behavior was observed in a recent study involving concrete resistance tests (16). However, due to the aggressiveness of the drying and wetting cycles in NaCl solution, the concentration of chloride ions (highly conductive) inside the specimens increased considerably after a certain period of time. Allied to this fact, the presence of small cracks caused by the drying/wetting cycle and by expansion due to the onset of the corrosion process caused the concrete resistance to decline again, reaching extremely low values at the end of the test. Silva (17) associated this fact to the samples higher moisture content.

It was found that until this inversion in behavior occurred (in this study, after five months of analysis), the samples with various red mud contents behaved similarly to the reference samples (without red mud), and even better at some points. However, the reference samples appeared to be more resistant to the aging of the experimental procedure, since their resistance declined less than the other samples.

Table 3 presents the results obtained for the electrode resistance, R_e (= R_p, Ω), as a function of the various red mud contents. According to some studies (12, 17), the rebar is in the process of corrosion if the diameter of semicircle formed at low frequencies is decreased, as observed in the Nyquist diagram. Therefore, the lower the R_e values the more advanced the corrosion process.

The results presented in Table 3 clearly show a reduction in R_e values, reaching differences of one order of magnitude between successive measurements, which stabilize at around 10^3 Ω (or kΩ). Several aspects of these results should be highlighted, as follows: i) The stabilization of these R_e values coincided with the inversion in the behavior of the R_b values, suggesting that this was in fact the moment when the corrosion process was at its highest level. ii) The reference specimens (0 % red mud content) reached this stabilization value earlier than the other samples (at three months of analysis), indicating that the corrosive process in the early stages was more pronounced in the reference samples than in the samples containing red mud. iii) The typical electrode resistance in an advanced corrosion process is in the order of kΩ.

The analysis of the EIS results revealed the evolution of the corrosion kinetics, identifying the moment when the corrosive process reached an advanced stage. However, the difficulties involved in their interpretation and the uncertainties about the parameters and characteristic ranges of the phenomena indicate that this technique still requires more in-depth study.

Electrical resistivity.

Electrical resistivity is a property widely used to monitor concrete structures because it is a nondestructive method and allows for external monitoring by means of embedded electrodes. This property is fundamentally related to fluid permeability and to ion diffusivity through concrete pores.

Several authors (18-22) have shown that electrical resistivity is related to the microstructural characteristics of the cement matrix, such as porosity, pore size distribution, pore connectivity, and the conductivity of the aqueous solution in the matrix. In this study, three specimens were prepared for each amount of red mud content, providing a total of six results (each specimen yielded two different measures because of the two electrodes embedded at different measuring depths).

Figure 9 shows the average results of the electrical resistivity of the reference specimens (0 %) and the specimens containing red mud additions (10 %, 20 % and 30 %). The specimens were kept in a moist chamber up to the age of 28 days, and the dotted lines in the figure represent the corrosion risk levels: high (<10 kΩ.cm), moderate (10 kΩ.cm to 50 kΩ.cm), low (50 kΩ.cm to 100 kΩ.cm), and insignificant (> 100 kΩ.cm), according to the COST 509.

All the samples showed increased electrical resistivity due to increased paste hydration and to the reduction of fluid concentration in concrete pores as the specimens became increasingly dry, making them less conductive. According to Santos (18), the conduction of electrical current through concrete occurs through continuous pores and microcracks that are present in the matrix and filled with water.

The behavior of the specimens differed significantly according to different moisture contents. Among the specimens that were kept in the moist chamber (up to 28 days), the samples containing red mud were more resistive than the reference samples (0 %). This effect continued to be visible in the first days after the specimens' removal from the moist chamber.

After drying the specimens, the reference samples showed a high increase in resistivity which exceeded that of the 40 to 80-day-old samples containing red mud. This effect can be explained by the high ionic concentration of red mud, which becomes more pronounced and active as the moisture content decreases when compared to reference samples. A similar behavior was observed by Whiting and Nagi (20).

The equivalent electrical conductivities of aqueous ions typically found in concrete pores were determined by Adamson *apud* Shi (23) and these values are presented in Table 4. As can be seen, the Na^+, OH^-, Ca^{2+} and K^+ ions in red mud are highly conductive, contributing to lower the resistivity of concrete when it loses moisture.

Another factor to be considered is the higher porosity of concrete specimens containing red mud, which contributes decisively in reducing resistivity. Although they showed lower resistivity values than the reference samples, the samples of concrete containing red mud showed values well above the limit considered as low corrosion probability (> 50 kΩ.cm). Hence, even if the presence of red mud does not prevent the occurrence of corrosion, it also cannot be considered harmful.

Another positive analysis factor is that the specimens containing red mud showed a higher resistivity in a humid environment, which is more conducive to corrosion. Unfortunately no measurements were taken of specimens kept moist throughout the experiment in order to verify if this behavior would be maintained.

Conclusions

This research led to the following conclusions:

- Electrochemical impedance spectroscopy (EIS) is a highly reproducible and powerful technique. However, its application is limited by the difficulties involved in interpreting EIS data and by the lack of internationally accepted criteria, indicating that this technique still lacks in-depth studies.

- The relationship between the arcs observed in the spectroscopy results and the characteristic relaxation frequency proved to be an interesting alternative for the analysis of heterogeneous and complex systems such as reinforced concrete, increasing the accuracy of measurements.

- The phenomena involved in reinforcement corrosion and the inherent characteristics of concrete are observed at low (10^{-3} Hz to 10 Hz) and medium (10^2 Hz to 10^6 Hz) frequencies, respectively. The typical electrode resistance of an advanced corrosion process is the order of kΩ (10^3 Ω).

- According to the Nyquist diagram, the rebar is undergoing corrosion when the semicircle formed at low frequencies is reduced.

- The EIS results indicated that the corrosion process was more advanced in the reference samples than in the samples containing red mud, indicating that this waste is a promising inhibitor of reinforced concrete corrosion;

- Electrical resistivity is a good indicator of the possible occurrence of chloride ion penetration. Thus, the higher the concrete's resistivity, the lower the penetration of chloride ions, and hence, the lower the probability of corrosion;

- The degree of saturation (humidity) of the concrete samples containing red mud appears to exert a considerable influence on the concrete's resistivity;

- The concrete specimens containing red mud presented higher resistivity in a humid environment, which is more favorable for corrosion.

References

(1) IBRAM – Brazilian Mining Association. **Bauxita**. Disponível em: <http://www.ibram.org.br/sites/1300/1382/00000033.pdf>. Acesso em: 15 mai. 2009.

(2) ROSKILL. **Bauxite.** Disponível em: <http://www.roskill.co.uk/index.html>. Acesso em: 08 mar. 2011.

(3) AMRITPHALE, S.S. *et al.* A novel process for making radiopaque materials using bauxite - Red mud. **Journal of the European Ceramic Society**. v. 27, n. 4, p. 1945-1951, 2007.

(4) KALKAN, E. Utilization of red mud as a stabilization material or the preparation of clay liners. **Engineering Geology**, v. 87, n. 6, p. 220-229, 2006.

(5) ASOKAN, P.; SAXEAN, M.; ASOLEKAR, S.R. Coal combustion residues-environmental implications and recycling potentials. **Resources, Conservation and Recycling**, v. 43, n. 3, p. 239-262, 2005.

(6) AMRITPHALE, S.S.; PATEL, M. Utilization of red mud, fly ash for manufacturing bricks with pyrophyllite. **Silicates Ind.,** v. 2, n. 3, p. 31-35, 1987.

(7) SGLAVO, V.M.; *et al.* Bauxite red mud in the ceramic industry. Part 2: production of clay based ceramics. **Journal of the European Ceramic Society**, v. 20, n. 3, p. 245-252, 2000.

(8) YALCIN, N.; SEVNIC, V. Utilization of bauxite waste in ceramic glazes. **Ceramics International,** v. 26, n. 5, p. 485-493, 2000.

(9) TSAKIRIDIS, P.E.; AGATZINI-LEONARDOU, S.; OUSTADAKIS, P. Red mud addition in the raw meal for the production of Portland cement clinker. **Journal of Hazardous Material**, v. 116, n. 1-2, p. 103-110, 2004.

(10) SINGH, M.; UPADHAYAY, S.N.; PRASAD, P.M. Preparation of iron rich cement from red mud. **Cement and Concrete Research**, v. 27, n. 7, p. 1037-1046, 1997.

(11) VERMOYAL, J.J.; FRICHET, A.; DESSEMOND, L.; HAMMOU, A. AC impedance study of corrosion films formed on zirconium based alloys. **Electrochimica Acta**, v. 45, n. 7, p. 1039–1048, 1999.

(12) MACHADO, M.A.G.T.C. **Inibidores de corrosão em concreto armado contra o ataque de agentes da chuva ácida.** 2004. 161p. Tese (Doutorado em construção civil), Universidade Federal de São Carlos, São Carlos, 2004.

(13) CHRISTENSEN, B.J.; et al. Impedance spectroscopy of hydrating cement-based materials: measurement, interpretation, and application. **Journal of the American Ceramic Society**, n. 77, v. 11, p. 2789-2804, 1994.

(14) COVERDALE, T.; *et al.* Interpretation of impedance spectroscopy of cement paste via computer modeling. **Journal of Materials Science**, v. 30, n. 20, p. 712-719, 1995.

(15) MAIA, L.F.; RODRIGUES, A.C.M. Electrical conductivity and relaxation frequency of lithium borosilicate glasses. **Solid State Ionics**, v. 168, n. 1-2, p. 87–92, 2004.

(16) RIBEIRO, D.V. **Influence of Red Mud Addition in Properties and Corrosibility of Reinforced Concrete.** 2010. 222p. Tese (Doutorado em Ciência e Engenharia de Materiais), Universidade Federal de São Carlos, São Carlos, 2010.

(17) SILVA, F.G. **Estudo de concretos de alto desempenho frente à ação de cloretos.** 2006. 218p. Tese (Doutorado em Ciência e Engenharia de Materiais) – Área de Interunidades em Ciência e Engenharia de Materiais, Universidade de São Paulo, São Carlos, 2006.

(18) SANTOS, L. **Avaliação da resistividade elétrica do concreto como parâmetro para a previsão da iniciação da corrosão induzida por cloretos em estruturas de concreto.** 161p. Dissertação (Mestrado em estruturas), Departamento de Estruturas, Universidade de Brasília, Brasília, 2006.

(19) POLDER, R.B. Test methods for on site measurement of resistivity of concrete - a RILEM TC-154 technical recommendation. **Construction and Building Materials**, v. 15, n. 2-3, p. 125-131, 2001.

(20) WHITING, D.A.; NAGI, M.A. **Electrical Resistivity of Concrete− A Literature Review**. Illinois, USA: Portland Cement Association, 2003. 57p. (R&D Serial No. 2457)

(21) BASHEER, P.A.M.; *et al.* Monitoring electrical resistance of concretes containing alternative cementitious materials to assess their resistance to chloride penetration. **Cement & Concrete Composites**, v. 24, n. 5, p. 437-449, 2002.

(22) MCCARTER, W.J.; STARRS, G.; CHRISP, T.M. Electrical conductivity, diffusion, and permeability of Portland cement-based mortars. **Cement and Concrete Research**, v. 30, n. 9, p. 1395-1400, 2000.

(23) SHI, C. Effect of mixing proportions of concrete on its electrical conductivity and the rapid chloride permeability test (ASTM C1202 or ASSHTO T277) results. **Cement and Concrete Research**, v. 34, n. 3, p. 537–545, 2004.

TABLES

Table 1 - Chemical composition of red mud estimated by XRF

Component	Al_2O_3	Fe_2O_3	Na_2O	CaO	SiO_2	K_2O	MnO	TiO_2	Others	LOI[a]
Content (wt. %)	19.87	19.85	7.35	4.61	14.34	1.87	0.21	2.66	1.01	27.20

[a] LOI = loss of ignition

Table 2 - EIS results of the corrosion resistance, R_b (Ω), of reinforced concrete without red mud (reference) and with different red mud contents (10 %, 20 % and 30 % (weight))

Age (Month)	**Corrosion Resistance, R_b (Ω)**			
	Reference (0 %)	**10 %**	**20 %**	**30 %**
1	9527.4	15453.0	13934.0	13763.0
2	7494.8	8224.7	9671.6	21304.7
3	15528.7	18036.7	25407.7	23312.8
5	31113.7	27623.3	64915.7	39640.9
7	6867.0	5536.7	3566.5	3387.6
9	7615.7	5079.7	6112.0	5731.2
11	7914.2	3239.3	3790.7	3586.3
13	13188.5	5983.1	4773.3	4580.9

Table 3 - EIS results of the electrode resistance, R_e (= R_p, Ω), of reinforced concrete without red mud (reference) and with different red mud contents (10 %, 20 % and 30 % (weight))

Age (Month)	**Electrode Resistance, $R_e = R_p$ (Ω)**			
	Reference (0 %)	**10 %**	**20 %**	**30 %**
1	1.99E+06	1.23E+06	3.33E+06	6.42E+06
2	1.79E+05	1.53E+05	2.79E+05	1.11E+06
3	7.66E+03	1.20E+04	1.08E+04	1.20E+05
5	5.44E+03	4.46E+03	3.16E+03	3.40E+03
7	2.24E+03	1.55E+03	1.93E+03	1.20E+03
9	3.14E+03	1.45E+03	1.50E+03	1.11E+03
11	3.18E+03	1.44E+03	1.34E+03	9.69E+02
13	3.09E+03	1.60E+03	2.68E+03	1.33E+03

Table 4 - Equivalent conductivity of aqueous ions in infinite concentrations at 25 °C (Adamson *apud* Shi (27))

Ion	Na^+	K^+	Ca^{2+}	SO_4^{2-}	OH^-	Cl^-
λ_0 ($m^{-1}\Omega^{-1}$)	0.00501	0.00735	0.00595	0.00798	0.0198	0.00763

FIGURES

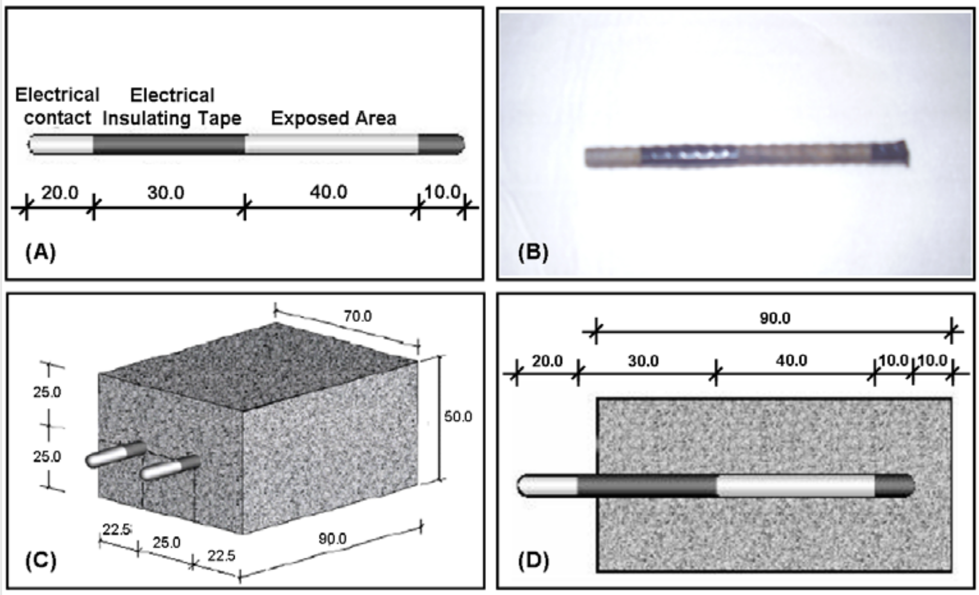

Figure 1 - (A) and (B) Scheme of the exposed rebar area (in mm); (C) sample dimensions (in mm); and (D) steel rebar positions in concrete samples.

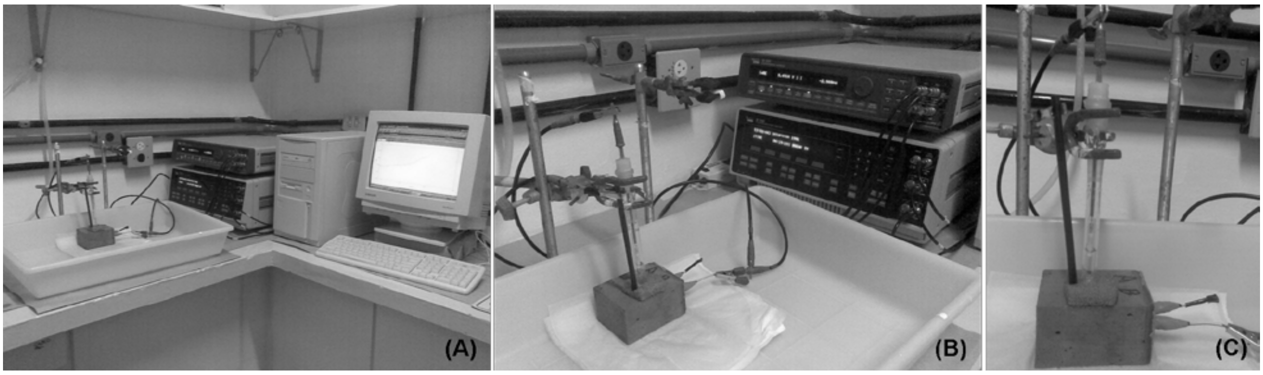

Figure 2 - Apparatus for measuring the corrosion process by electrochemical impedance spectroscopy (EIS).

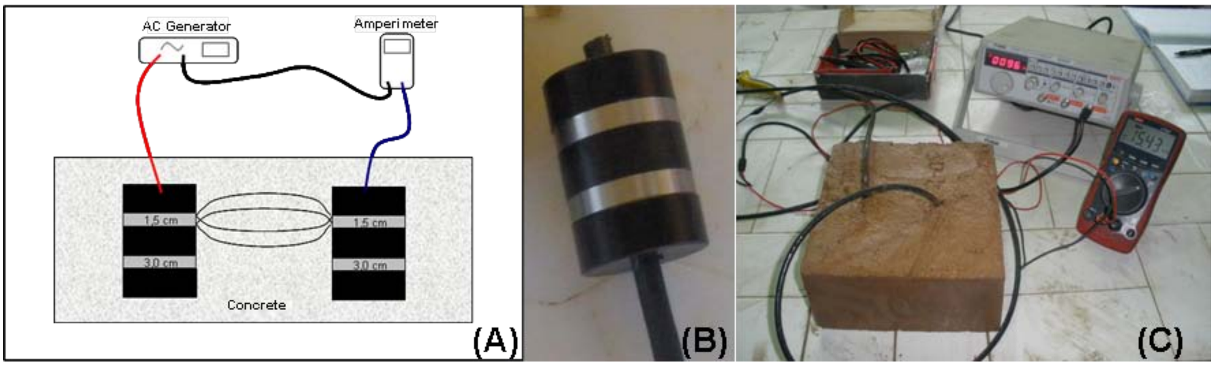

Figure 3 - (A) Schematic diagram of the measurement of concrete electrical resistance, (B) electrical probe and (C) electrical current measure.

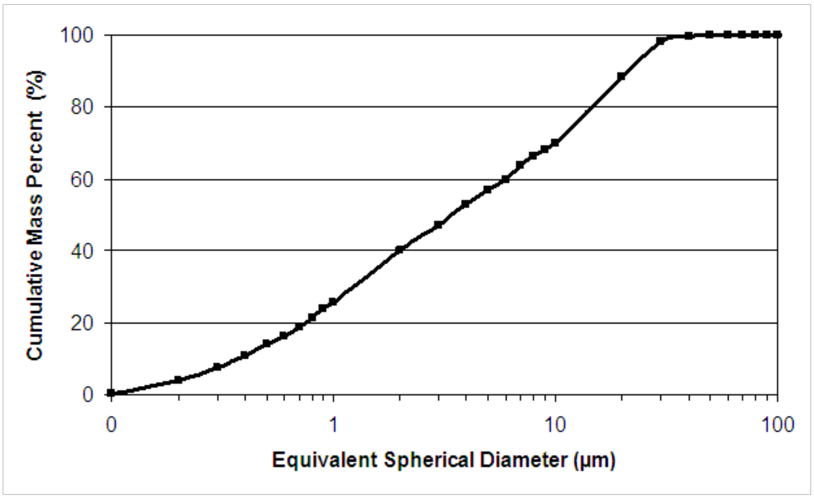

Figure 4 - Particle size distribution of the dry red mud

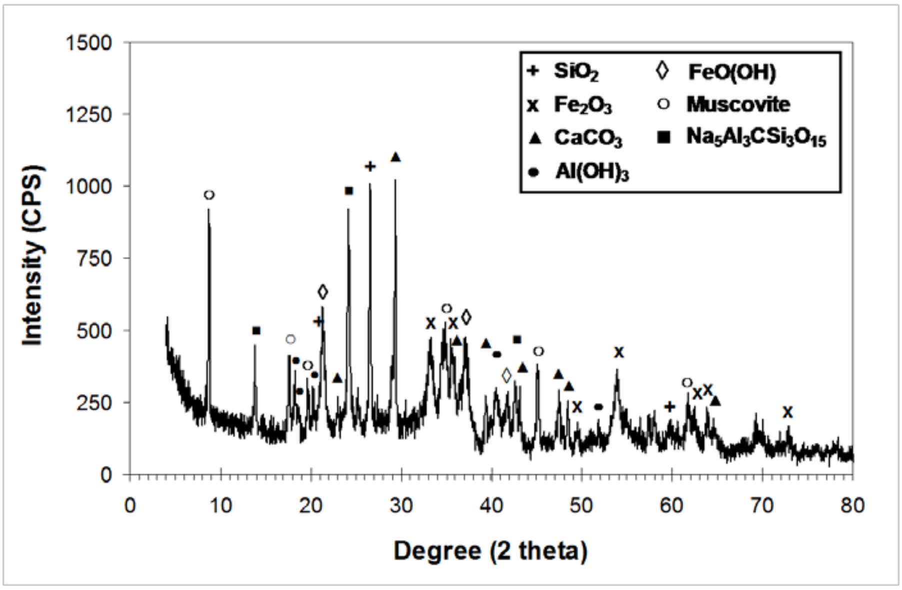

Figure 5 - X-ray diffraction (XRD) pattern of dry red mud.

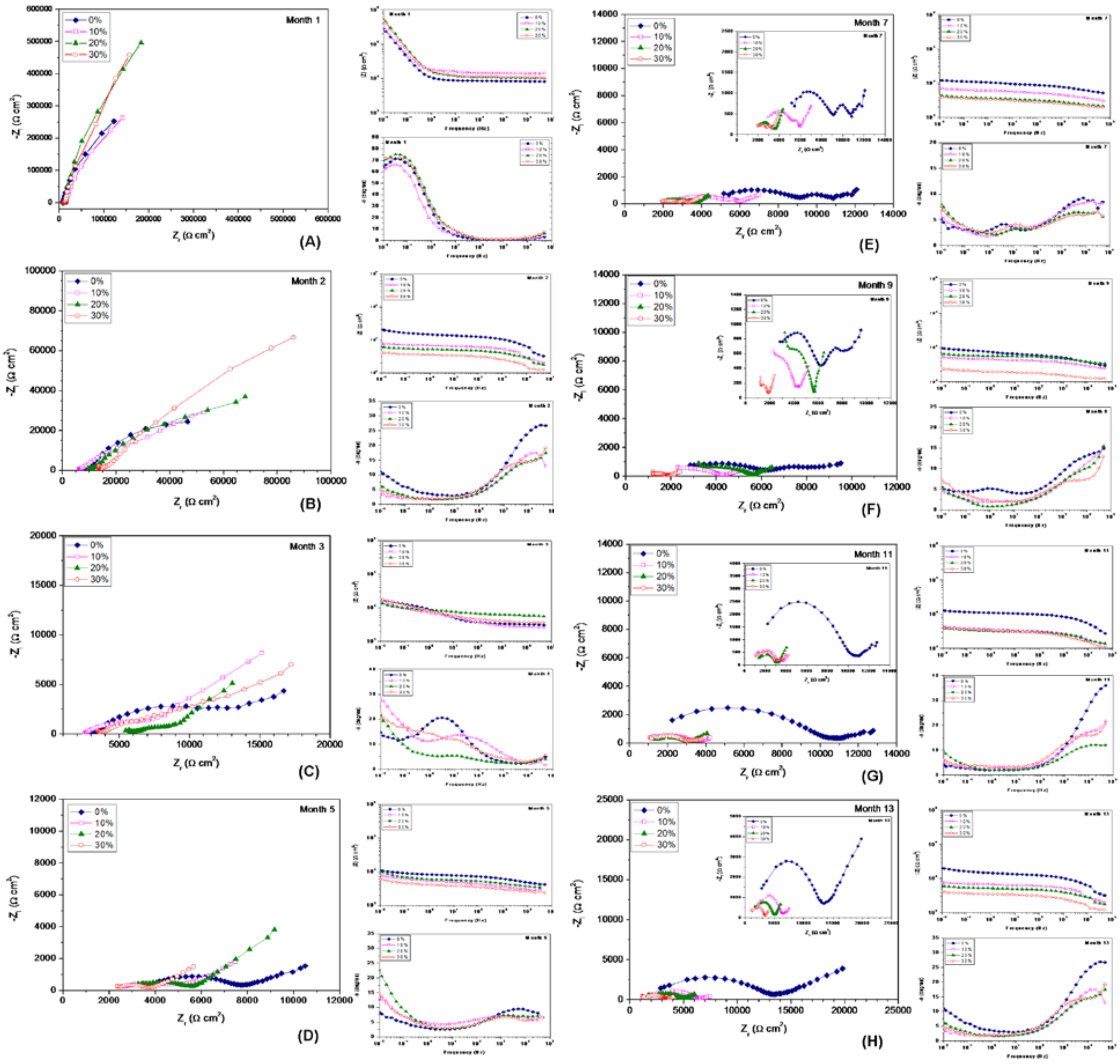

Figure 6 - Impedance spectra (Nyquist and Bode diagrams) of concrete samples without red mud and with red mud contents of 10 %, 20 % and 30 % (weight): (A) 1 month; (B) 2 months; (C) 3 months; and (D) 5 months; (E) 7 months; (F) 9 months; (G) 11 months; and (H) 13 months of age.

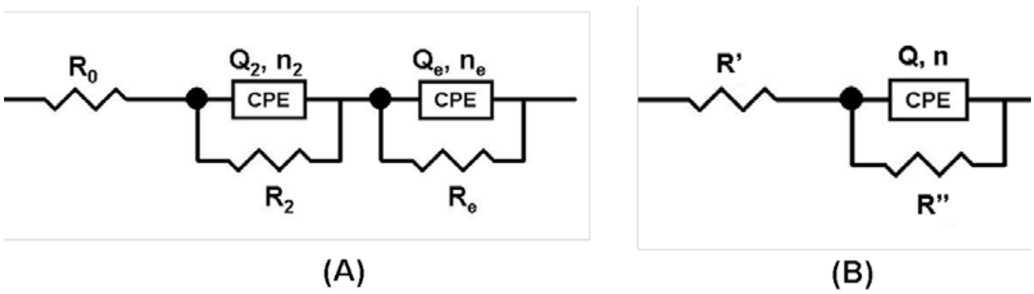

Figure 7 - Equivalent electrical circuits proposed for the steel-concrete interface, based on (A) a general analysis, and (B) analysis of individual arcs (simplified circuit).

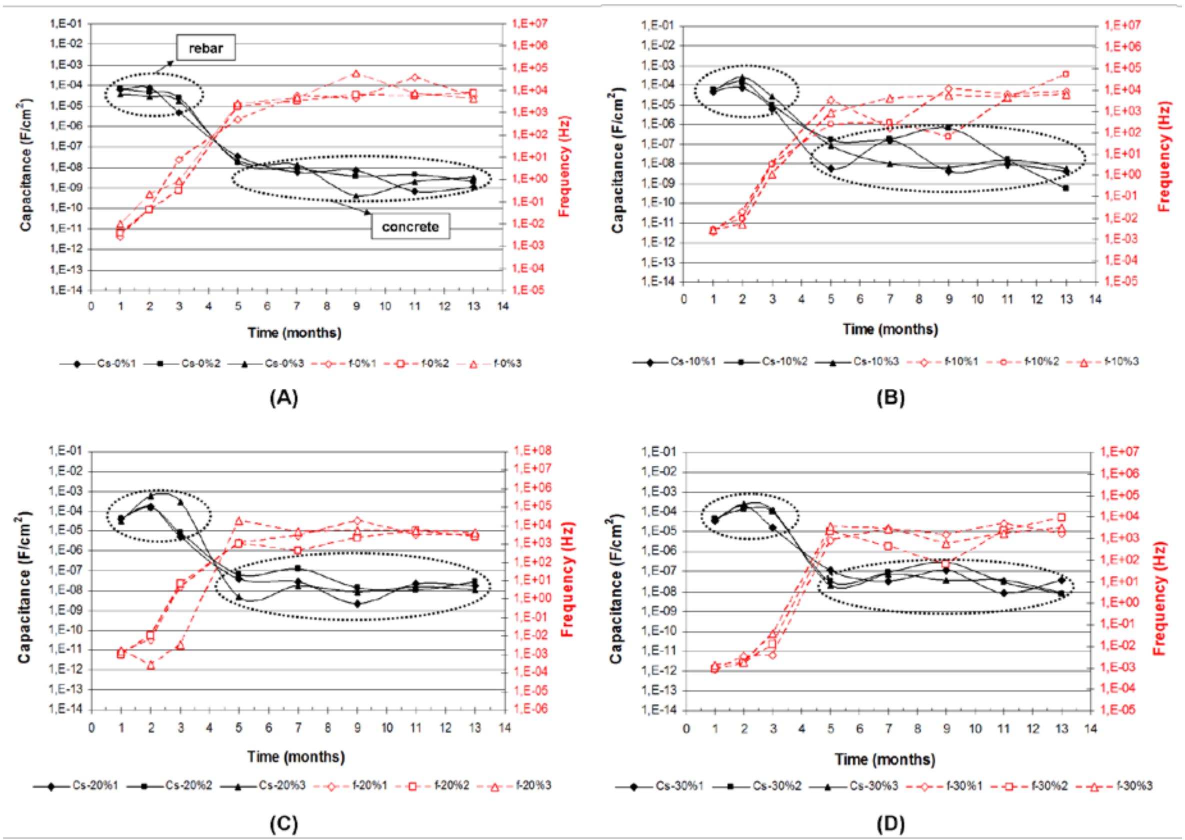

Figure 8 - Examples of correlation between the characteristic capacitance and frequency of each of the phenomena observed by EIS for (A) reference concrete samples, and for samples with varying red mud contents: (B) 10 %, (C) 20 % and (D) 30 % (weight).

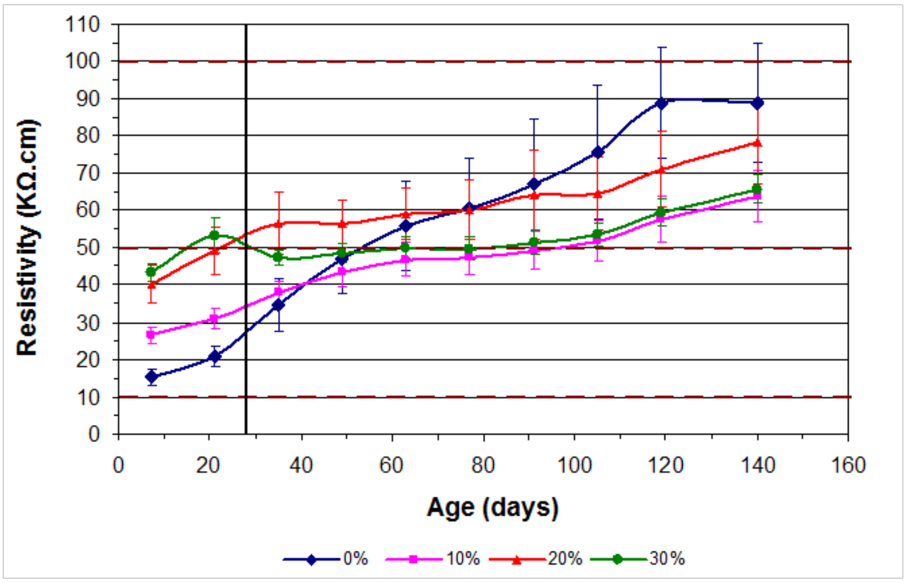

Figure 9 - Electrical resistivity of concrete specimens containing red mud, as a function of age.